Analysis of fluid flow in a cylindrical tube using fiber Bragg grating

Agam Muhammad Maulana[1],*, Khaikal Ramadhan[2], Dedi Irawan[3]

[1]Department of Physics, Universitas Riau, Pekanbaru 28293, Indonesia
[2]Department of Physics, Institut Teknologi Bandung, Bandung 40132, Indonesia
[3]Department of Physics Education, Universitas Riau, Pekanbaru 28293, Indonesia

ABSTRACT

Fiber Bragg grating (FBG) is an optical sensor component that has better performance than other optical and electronic components. FBG has a very high sensitivity to changes in temperature and strain, is small in size, and is resistant to electromagnetic wave interference and multiplexing. In this study, FBG is used to monitor the fluid flow rate in a pipe by analyzing changes in the output power generated by the FBG. This research was designed by varying the pipe diameter, measurement position, and fluid flow rate. The diameters of the pipes used are 5.95, 7.01, 8.79, and 10.32 mm. The fluid flow rate that passes through each pipe is also varied. The measuring position is placed at 1/3 2/3, and 3/3 pipe diameter. The fluid flow rate and the output power generated by this FBG are measured using an anemometer and optical power meter respectively. The FBG used in this study has a center wavelength of 1310 nm and 1550 nm. In this study, the value of power generated from pipe 1 of position 1 FBG with a wavelength of 1550 nm is 15.1 dBm, while at a wavelength of 1310 nm is -26.23 dBm which indicates that the power generated from FBG with a wavelength of 1310 is the biggest. The speeds obtained at pipe position 1 from the anemometer measurements are 0.79, 1, 1.82, and 2.22 m/s which are directly proportional to the power generated at the 1550 wavelength FBG, -15.1, -15.12, -15.47, and -15.43 dBm, respectively. So it can be concluded that the greater the speed generated by the fluid flow, the greater the power generated.

ARTICLE INFO

* Corresponding Author

E-mail address: agam.mohammad3325@student.unri.ac.id

1. INTRODUCTION

In the oil and gas industry, technology is needed that can monitor the speed of fluid flow in pipes and can also monitor problems that occur in pipes [1]. Oil and gas pipelines experience problems such as gas leaks [2], blocked flow [3], and other problems that can disrupt fluid flow in the pipe [4]. Because of this problem, fiber optic technology, especially fiber Bragg gratings (FBG), can be used as an alternative solution in monitoring fluid flow conditions in gas pipes. FBG sensors can detect temperature [5] and strain [6] for even very small changes. Apart from that, FBG also has advantages such as small size [7], resistance to electromagnetic interference [8], multiplexing [9], long-distance sensing [10], very sensitivity to environmental changes [11], and very fast sensing when compared to electronic sensors [12].

Several researchers have developed FBG sensors for many applications such as simultaneous temperature and strain sensing [13, 14], high temperature sensing [15, 16], extreme weather sensing [17], cryogenic temperature sensing [18], and sensing for biomedical applications [19]. in processing FBG signals it has also been reported by many researchers to provide sensitive and accurate optical signals such as providing an apodization profile on the FBG [20-22]. apodization is a technique to narrow the full-width half maximum and also increase the difference between sidelobe left and sidelobe right [23].

FBG consists of a core, cladding and usually also coated with a coating [24-26]. What differentiates FBG from ordinary fiber is the presence of a lattice whose refractive index changes periodically. FBG lattices also have many sizes such as slanted lattices, chirps, superstructures, etc [27-29]. The use of FBG as a sensor has been widely reported by many researchers, but very few have applied it to fluid flow. Changes in fluid flow that are not uniform make it difficult to determine the characteristics of the resulting optical signal [30].

In this paper, experiments were carried out to determine the characteristics of the output signal produced by the FBG due to changes in fluid flow speed. The fluid flow speed is measured using an anemometer and then a hole is made in the pipe to insert the FBG inside. Next, the output power results are measured using an optical power meter (OPM).

2. LITERATURE REVIEW

Optical fiber is a light transmission medium whose constituent material is glass or plastic. Optical fibers have various diameters, consisting of a core and a cladding. Optical fibers are used in many applications such as optical communications, optical sensors, and optical monitoring. An American scientist was the first to introduce optical fiber with the name Charles Kao, in his extraordinary discovery he received the Nobel Prize in Physics in 2009. Since the discovery of optical fiber, developments in the world of telecommunications have experienced very rapid developments starting from alternative uses of materials and uses. in all scientific fields [20].

Optical fibers are composed of a coating, core, and cladding with different refractive indices. The refractive index of the core has a value greater than the refractive index of the sheath so light is always reflected in the core and light refraction does not occur. As in Figure 1 below, the structure of an optical fiber is shown [21].
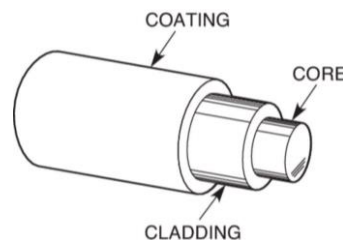

Figure 1. Optical fiber structure.

This jacket layer functions to protect the optical fiber from external pressure and also protects it from damage. Apart from that, the jacket also functions to reduce light coming out of the core and sheath into the surrounding environment. This part is not involved in the process of transmitting light which is an electromagnetic wave. The core is a vital part of an optical fiber. Most of the light is transmitted through this layer. The core is made of plastic or glass materials such as silica (SiO_2), Topaz cyclic olefin copolymer [20], and others. The fiber optic core has a diameter of about 8 to 200 µm. and a refractive index that is greater than the refractive index of the sheath. The sheath is a layer that covers the core with a lower refractive index compared to the core. The function of the sheath is to reflect electromagnetic waves which limit light from escaping into the environment [22].

Approximately, the layer of this casing can be made of glass or plastic material which has a lower refractive index than the core refractive index. The sheath has a diameter of over 250 – 400 µm. Based on the mode, optical fiber can be divided into 2, namely single-mode fiber (SMF) and multiple mode (multimode fiber). SMF has one mode which has a core diameter of around 8 µm to 12 µm and a sleeve diameter of 125 µm. SMF has a small distribution time and fewer losses compared to other types of distribution. This SMF can only transmit signals in one mode because it only transmits signals in the main mode to prevent chromatic dispersion [23]. Multimode fiber has a cable core of around 50 to 200 µm, using a wavelength of 850 or 1300 nm. It is called multi-mode because this type of optical fiber allows hundreds of modes of light to be spread through the fiber simultaneously. This type of fiber usually has poor transmission performance, narrow bandwidth, and small transmission capacity.

2.1. Development of Optical Fiber

As time goes by, the development of fiber optics begins to be seen, from those initially used only in the field of telecommunications but can also be used as sensors known as fiber optic sensors, fiber optic sensors can be grouped into extrinsic fiber optic sensors, intrinsic fiber optic sensors and evanescent sensors which in general The working principle of a fiber optic sensor is that the nature of the optical fiber is photoelastic so it is very sensitive to changes in the environment. The quantities that can usually be measured in a fiber optic sensor are strain and temperature [20].

2.2. FBG

FBG is an optical fiber with a refractive index that changes periodically due to the presence of a grating at a certain distance. This is because the optical fiber is photosensitive, that is, the refractive index of the core can change with exposure to ultraviolet light which is large enough. The basic material in manufacturing FBG is germanium. The following Figure 2 shows the schematic of an FBG, where the FBG acts like an optical filter, namely reflecting the central wavelength or Bragg wavelength and transmitting the rest [21].
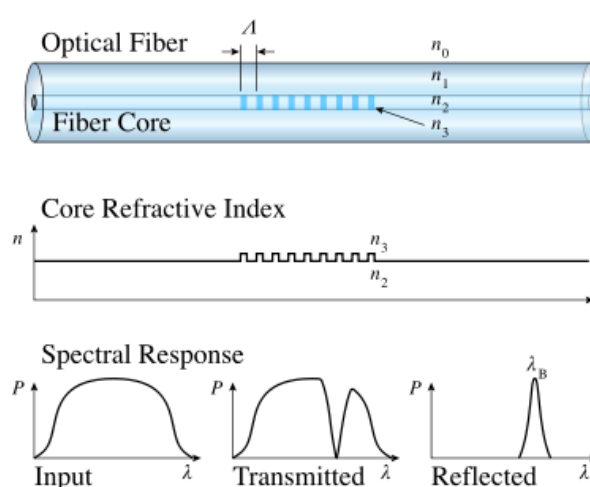

Figure 2. Working principles of FBG.

FBG has a lattice whose refractive index changes periodically, because of this the FBG can reflect certain wavelengths, a working system like this makes FBG used in optical technology, such as in optical communications to filter signals for temperature and strain monitoring.

3. RESEARCH METHODS

In the initial stages of the research, clamps and stands were prepared to support the pipe and anemometer so that they remained static. The pipes used are 4 pipes which have different dimensions with diameters of 5.95 mm, 7.01 mm, 8.79 mm, and 10.32 mm respectively, and the length of each pipe is 1 meter, the pipes are given a small hole in the middle of each pipe which functions to insert the FBG into the pipe and adjust its position. Pipe selection is based on the availability of experimental equipment and is also adjusted to the dimensions of the FBG that will be associated with the tool.

In this hole, the FBG is inserted by making a notch right on the FBG and then covering it again with paper tape, one end of the FBG will be attached to a laser and the other end will be attached to an OPM to determine the laser output power. This system will later be varied based on fluid speed, position of the FBG, and type of FBG. At the base of the pipe, fluid will flow which will be assisted by an air pump, and at the other end of the pipe, an anemometer will be attached to measure the speed of the fluid.

After the system is designed and implemented. OPM is used to measure the output power of each variation, such as different speeds and different positions. and the OPM will display the output power for each different speed and the output power for different positions will be measured. The

FBG outputs power for 3 different positions on the pipe and 4 air speeds on the FBG. From this data, you will be able to see a graph of the FBG output power for a certain position and speed.

4. RESULTS AND DISCUSSIONS

Pipe 1 has a diameter of 5.95 mm, and is the smallest pipe diameter among the other pipes. On pipe 1, four-speed variations were measured, respectively, the speed results obtained by the anemometer were 0.79 m/s, 1 m/s, 1.82 m/s, and 2.22 m/s. When measuring speed variations, power monitoring is carried out at 3 positions, after being exposed to laser light with a power of 1 mW on Pipe 1 for 3 different positions, the output power for the FBG is obtained with a wavelength of 1310 nm and 1550 nm in Figure 3. experiments were carried out by ensuring the same speed for different positions and pipes. The output power is measured using OPM. The distribution of output power produced in pipe 1 for 2 different positions can be seen in Figure 3.

FBG 1310 nm   FBG 1550 nm
(a) Pipe 1 Position 1 diameter 5.95 mm

FBG 1310 nm   FBG 1550 nm
(b) Pipe 1 Position 2 diameter 5.95 mm

FBG 1310 nm   FBG 1550 nm
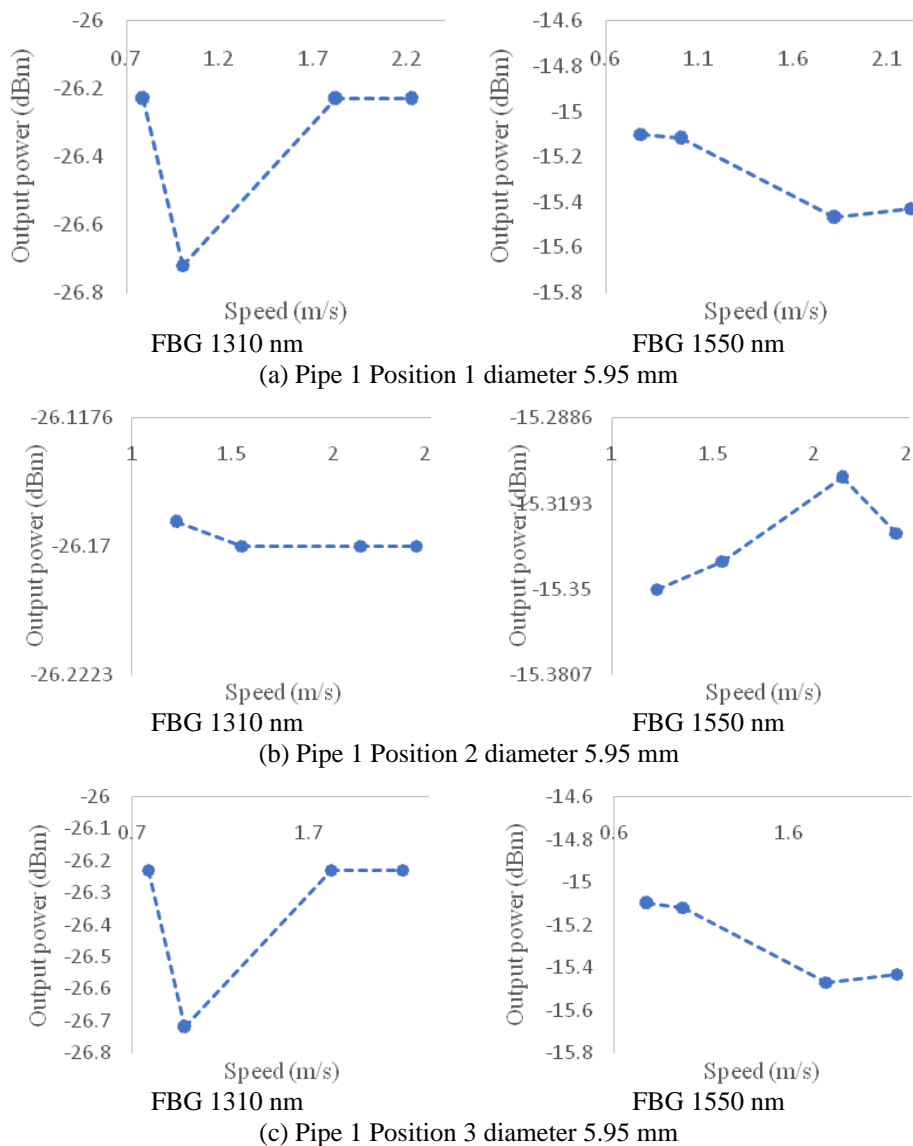(c) Pipe 1 Position 3 diameter 5.95 mm

Figure 3. Output power for pipe 1: (a) position 1; (b) position 2; and (c) position 3.

Figure 3 (a) on pipe position 1 which forms a graph of the comparison of ΔP to v, shows that the faster the speed produced by the fluid, the greater the power produced by the FBG on pipe 1 position 1. The resulting power data is -15.43 dBm at a speed of 2.22 m/s The speed obtained is based on the fluid from the pump which is getting bigger due to the small dimensions of the pipe. In contrast

to the power produced from a wavelength of 1550 nm at a wavelength of 1310 nm the power is less constant, this condition can be seen in the table where at speeds of 0.79 m/s, 1.82 m/s, and 2.22 m/s we get the same power is -26.23 dBm and at a speed of 1 m/s, the power is -26.72 dBm. When the experiment was carried out the FBG was less responsive to the given speed.

In Figure 3 (b) in pipe position 2 which forms almost the same graph, all the power is produced from a wavelength of 1310 nm with different speeds at a speed of 1.22 m/s the power produced by the FBG is -26.16 dBm while for The other 3 speeds get a power of -26.17 dBm, respectively, the speeds obtained are 1.55m/s, 2.14 m/s, and 2.41 m/s. In the process of fluid speed, the power value produced is not much different, causing a very slight comparison, but if rounded to two decimal places after the comma it becomes the same value. At a wavelength of 1550, the power obtained significantly increases when the speed also increases. Based on the image above, the speed and power obtained are a speed of 1.22 m/s with a power of -15.25 dBm, then 1.55 m/s with a power of -15.34 dBm, 2.14 m/s with power of -15.31 dBm, and 2.41 m/s with power of -15.33 dBm.

Furthermore, in Figure 3 (c), precisely at position 3 at the base of the pipe there is no different value from position 1 at the end of the pipe because the pipe is cylindrical. When the pipe is rotated there is no significant difference in position of the pipe. This is the same situation at these two wavelengths and there is a significant difference in the power produced because the power determination is different from that carried out in this experiment due to the FBG being less stable.

5. CONCLUSION

After conducting a study and analysis of the data from the research conducted, it can be concluded that the speed produced by the fluid flow in the cylinder tube affects the power value obtained in the FBG with speeds of 0.79 m/s, 1 m/s, 1.82 m /s, and 2.22 m/s affect the FBG with a wavelength of 1550 nm by -15.1 dBm, -15.12 dBm, -15.47 dBm and -15.43 dBm and this also indicates that the greater the speed value the greater the power produced.

REFERENCES

[1] Ramadan, K. M., Kamil, M., Tlili, I., & Qisieh, O. (2021). Analysis of thermal creep effects on fluid flow and heat transfer in a microchannel gas heating. *J. Therm. Sci. Eng. Appl.*, **13**(6).

[2] Wang, K., Hu, Y., Qin, M., Liu, G., Li, Y., & Wang, G. (2021). A leakage particle–wall impingement based vibro-acoustic characterization of the leaked sand–gas pipe flow. *Particuology*, **55**, 84–93.

[3] Wang, W., Mao, X., Liang, H., Yang, D., Zhang, J., & Liu, S. (2021). Experimental research on in-pipe leaks detection of acoustic signature in gas pipelines based on the artificial neural network. *Measurement*, **183**, 109875.

[4] Christos, S. C., Fotis, G., Nektarios, G., Dimitris, R., Areti, P., & Dimitrios, S. (2021). Autonomous low-cost wireless sensor platform for leakage detection in oil and gas pipes. *2021 10th International Conference on Modern Circuits and Systems Technologies (MOCAST)*, 1–4.

[5] Ye, Z., Li, Z., Dai, J., Qin, Y., Wang, G., Yuan, Z., & Yang, M. (2021). Hydrogen sensing performance investigations with optical heating and sensing element surface modification. *International Journal of Hydrogen Energy*, **46**(1), 1411–1419.

[6] Cavaleiro, P. M., Araujo, F. M., Ferreira, L. A., Santos, J. L., & Farahi, F. (1999). Simultaneous measurement of strain and temperature using Bragg gratings written in germanosilicate and boron-codoped germanosilicate fibers. *IEEE Photonics Technology Letters*, **11**(12), 1635–1637.

[7] Barbarin, Y., Lefrançois, A., Chuzeville, V., Magne, S., Jacquet, L., Elia, T., Woirin, K., Collet, C., Osmont, A., & Luc, J. (2020). Development of a shock and detonation velocity measurement system using chirped fiber Bragg gratings. *Sensors*, **20**(4), 1026.

[8] Perezcampos Mayoral, C., Gutiérrez Gutiérrez, J., Cano Pérez, J. L., Vargas Treviño, M., Gallegos Velasco, I. B., Hernández Cruz, P. A., Torres Rosas, R., Tepech Carrillo, L., Arnaud Ríos, J., Apreza, E. L., & Rojas Laguna, R. (2021). Fiber optic sensors for vital signs monitoring. A review of its practicality in the health field. *Biosensors*, **11**(2), 58.

[9] Fan, X., Ou, Z., Zhang, L., Zhang, R., Yuan, C., Deng, G., Wang, Y., Song, H., You, L., Liu, Y., Guo, G., & Zhou, Q. (2022). Dense temporally multiplexed fiber bragg grating sensing based on single-photon detection. *Journal of Lightwave Technology*, **40**(13), 4458–4466.

[10] Hanto, D. & Iiyama, K. (2019). Low-cost interrogation of long-distance and multipoint FBG sensor using incoherent-FMCW optical ranging system. *IEEE Sensors Journal*, **20**(7), 3599.

[11] Markowski, K., Jędrzejewski, K., Marzęcki, M., & Osuch, T. (2017). Linearly chirped tapered fiber-Bragg-grating-based Fabry–Perot cavity and its application in simultaneous strain and temperature measurement. *Optics Letters*, **42**(7), 1464–1467.

[12] Yan, G., Zhang, A. P., Ma, G., Wang, B., Kim, B., Im, J., He, S., & Chung, Y. (2011). Fiber-optic acetylene gas sensor based on microstructured optical fiber Bragg gratings. *IEEE Photonics Technology Letters*, **23**(21), 1588–1590.

[13] Chen, G., Liu, L., Jia, H., Yu, J., Xu, L., & Wang, W. (2004). Simultaneous strain and temperature measurements with fiber Bragg grating written in novel Hi-Bi optical fiber. *IEEE Photonics Technology Letters*, **16**(1), 221–223.

[14] Mansoursamaei, M. & Malakzadeh, A. (2021). Simultaneous measurement of temperature and strain using a single fiber bragg grating on a tilted cantilever beam. *Optical Review*, **28**, 289.

[15] Eid, M. M., Seliem, A. S., Rashed, A. Z., Mohammed, A. E. N. A., Ali, M. Y., & Abaza, S. S. (2021). High sensitivity sapphire FBG temperature sensors for the signal processing of data communications technology. *Indones. J. Electr. Eng. Comput. Sci.*, **21**, 1567–74.

[16] Kumar, J., Singh, G., Saxena, M. K., Prakash, O., Dixit, S. K., & Nakhe, S. V. (2020). Development and studies on FBG temperature sensor for applications in nuclear fuel cycle facilities. *IEEE Sensors Journal*, **21**(6), 7613–7619.

[17] Yang, S., Homa, D., Heyl, H., Theis, L., Beach, J., Dudding, B., Acord, G., Taylor, D., Pickrell, G., & Wang, A. (2019). Application of sapphire-fiber-Bragg-grating-based multi-point temperature sensor in boilers at a commercial power plant. *Sensors*, **19**(14), 3211.

[18] Hsu, C. Y., Chiang, C. C., Hsieh, T. S., Hsu, H. C., Tsai, L., & Hou, C. H. (2021). Study of fiber Bragg gratings with TiN-coated for cryogenic temperature measurement. *Optics and Laser Technology*, **136**, 106768.

[19] Fajkus, M., Nedoma, J., Martinek, R., Vasinek, V., Nazeran, H., & Siska, P. (2017). A non-invasive multichannel hybrid fiber-optic sensor system for vital sign monitoring. *Sensors*, **17**(1).

[20] Saktioto, T., Ramadhan, K., Soerbakti, Y., Syahputra, R. F., Irawan, D., & Okfalisa, O. (2021). Apodization sensor performance for TOPAS fiber Bragg grating. *TELKOMNIKA*, **19**(6), 1982.

[21] Saktioto, T., Ramadhan, K., Soerbakti, Y., & Irawan, D. (2021). Integration of chirping and apodization of Topas materials for improving the performance of fiber Bragg grating sensors. *Journal of Physics: Conference Series*, **2049**(1), 012001.

[22] Ramadhan, K., Saktioto, Syahputra, R. F., Soerbakti, Y., & Fauzan, M. (2020). Dispersi multi-layer pada inti serat optik moda tunggal. *Seminar Nasional Fisika Universitas Riau V*, **5**(1), 1–5.

[23] Irawan, D., Azhar, A., & Ramadhan, K. (2022). High-performance compensation dispersion with apodization chirped fiber bragg grating for fiber communication system. *Jurnal Penelitian Pendidikan IPA*, **8**(2), 992–999.

[24] Sengupta, D., Shankar, M. S., Reddy, P. S., Prasad, R. S., Narayana, K. S., & Kishore, P. (2011). An improved low temperature sensing using PMMA coated FBG. *Asia Communications and Photonics Conference and Exhibition*, 831103.

[25] Ramadhan, K., Irawan, D., & Yupapin, P. (2023). Core multi-layer dispersion on single-mode optical fiber. *Science, Technology and Communication Journal*, **3**(3), 89–94.

[26] Saktioto, S., Defrianto, D., Thoibah, A., Soerbakti, Y., Syahputra, R. F., Syamsudhuha, S., Irawan, D., Hairi, H., Okfalisa, O., & Amelia, R. (2023). Simplified kinetic model of heart pressure for human dynamical blood flow. *Indones. J. Electr. Eng. Inform.*, **11**(3), 870-882.

[27] Saktioto, Rahmat, I., & Juandi. (2016). Penentuan rugi-rugi kelengkungan fiber optik mode tunggal secara komputasi. *Indonesian Physics Communication*, **13**(13), 896–900.

[28] Hikma, N., Saktioto, T., & Soerbakti, Y. (2023). Vibration analysis of diaphragmatic breathing activity using single-mode fiber and fiber Bragg grating. *AIP Conference Proceedings*, **2858**(1).

[29] Defrianto, D., Pratama, N., & Malik, U. (2023). Determination of the shadow zone area in the ocean computationally by simulating the propagation of acoustic rays. *Sintechcom*, **3**(2), 59–64.

[30] Saktioto, S., Defrianto, D., Hikma, N., Soerbakti, Y., Irawan, D., Okfalisa, O., Widiyatmoko, B., & Hanto, D. (2022). External perspective of lung airflow model via diaphragm breathing sensor using fiber optic elastic belt. *The 4th Al-Noor International Conference for Science and Technology*, **4**(1), 1014.